Available online at www.sciencedirect.com
SCIENCE DIRECT®
Journal of Nuclear Materials 337–339 (2005) 1101–1105
journal of nuclear materials
www.elsevier.com/locate/jnucmat

Neutral helium line emission for edge plasma conditions

F.B. Rosmej [a,*], R. Stamm [a], S. Fritzsche [c], H. Capes [b], M. Koubiti [a], Y. Marandet [a], V.S. Lisitsa [d], N. Ohno [e], S. Takamura [f], D. Nishijima [g]

[a] PIIM-UMR 6633 CNRS/Université de Provence, centre St-Jérôme, 13397 Marseille, France
[b] DRFC, Association Euratom-CEA, 13108 Saint Paul lez Durance Cedex, France
[c] Department of Physics, University Kassel, Heinrich-Plett-Str. 40, D-34132 Kassel, Germany
[d] Russian Research Center 'Kurchatov Institute', 123182 Moscow, Russia
[e] EcoTopia Science Institute, Nagoya University, Japan
[f] Department of Energy Engineering and Science, Nagoya University, Japan
[g] Max-Planck Institut für Plasmaphysik, D-85748 Garching, Germany

Abstract

A diagnostic method for the determination of the neutral helium diffusion coefficient in the edge of magnetically confined fusion plasmas is developed on the basis of emission spectroscopy and population kinetics. The new collisional-radiative numerical code SOPHIA showed that intercombination transitions are extremely important to describe the qualitative and quantitative behaviour of the line emission and the population flow in diffusive plasmas. Corresponding simulations relevant for edge plasma conditions and the NAGDIS-II plasma simulator are discussed.

PACS: 32.70.Fw; 52.55.Fa; 52.25.Rv; 52.25.Vy
Keywords: Divertor plasma; Diffusion; Edge modelling; Radiation; Helium; Neutrals; JET; NAGDIS-II; Spectroscopy

1. Introduction

Detached plasmas provide a promising method for reducing the heat flux of plasma facing components and their investigation is an important ITER design activity. Recombination processes are responsible for the plasma detachment and the spectroscopic investigation of the corresponding radiation emission is therefore of great interest [e.g., [1–3]]. However, molecular recombination processes involved are very complex (e.g., vibrationally excited hydrogen molecules) and it is desirable to avoid them as they are difficult to model. For this reason the analysis of the neutral helium emission to probe edge plasma conditions is much more advantageous.

The analysis of the radiation emission originating from the various elements and ionisation stages is of great interest, because it provides the possibility for a wide and unique characterization of the plasma: e.g., temperature, density, diffusion, charge exchange, fields, temporal and spatial variations, turbulence and fluctuation analysis. Moreover, a large impact from the spectroscopic analysis stems from the fact, that it is based essentially on a collisional-radiative approach and therefore provides a plasma model independent information.

* Corresponding author.
E-mail addresses: rosmej@piima1.univ-mrs.fr (F.B. Rosmej), roland.stamm@piimdgp.univ-mrs.fr (R. Stamm).

0022-3115/$ - see front matter © 2004 Elsevier B.V. All rights reserved.
doi:10.1016/j.jnucmat.2004.10.141

In order to study diffusion and radiation transport processes under detached plasma conditions through the perturbation of the neutral helium spectral distribution we have developed a new collisional-radiative numerical simulation code SOPHIA [4]. Simulations relevant for the interpretation of the neutral helium lines in edge plasma conditions [5] and the NAGDIS-II plasma simulator [1] are discussed.

2. Experimental spectra of neutral helium line emission

Fig. 1 shows the emission spectra [1] of neutral helium obtained from the NAGDIS-II plasma simulator [6] which is able to simulate relevant regimes of magnetic fusion for edge plasma conditions. The wavelength range of 350–365 nm contains the Rydberg-series of the triplet lines $1s2p\,^3P$–$1snd\,^3D$ and the singlet line $1s2s\,^1S$–$1s5p\,^1P_1$. The spectra are dispersed by a grating with 1200 grooves per mm. As indicated by arrows in Fig. 1(a) and (b), there are observed strong variations

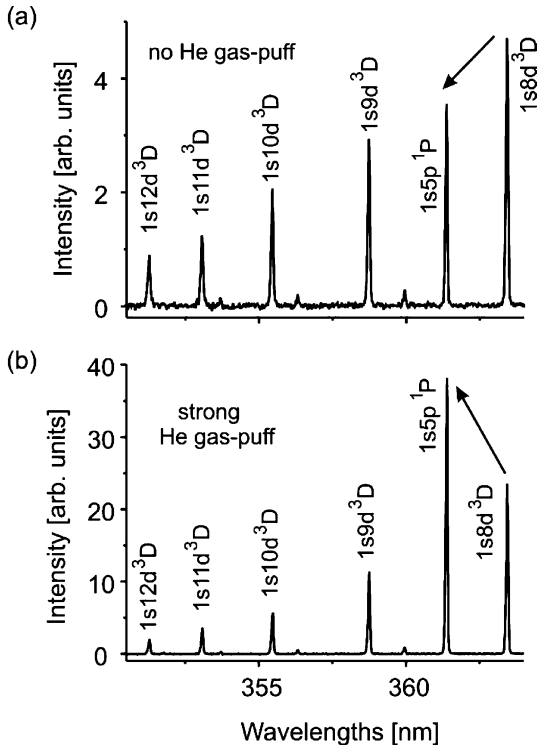

Fig. 1. Neutral helium experimental spectra from the NAGDIS-II divertor plasma simulator, (a) at neutral He pressure of 0.573 Pa without secondary He gas puffing, # A2364AD1, (b) at neutral He pressure of 2.84 Pa with secondary He gas puffing, # A2364AD20. The strong relative variation of the singlet $1s2s^0$–$1s5p\,^1P_1$ line is indicated by arrows.

of the $1s2s\,^1S$–$1s5p\,^1P_1$ line. The spectrum of Fig. 1(a) was obtained without secondary He gas-puff (corresponding to weakly detached plasmas) whereas the spectrum presented in Fig. 1(b) was obtained with a strong secondary gas-puff (corresponding to deeply detached plasmas). We note that non-equilibrium values of the singlet/triplet intensity ratio and their variations have also been observed at JET [5].

Theoretical simulations with the SOPHIA-code show, that the observed singlet and triplet lines shown in Fig. 1 are sensitive to diffusion processes [5]. It is therefore of great interest to study the line variations for the investigation of different plasma regimes like attached or detached plasmas under well controlled conditions.

3. Simulation of helium emission: diffusion and radiation transport

Simulation of the line radiation emission requires the determination of a large set of atomic and ionic populations. In more general terms the atomic-level population densities are determined from a system of rate equations:

$$\frac{\mathrm{d}n_j}{\mathrm{d}t} = \sum_{i=1}^{N} n_i\{W_{ij} + A_{ij}\Lambda_{ij}\} - n_j \sum_{k=1}^{N}\{W_{jk} + A_{jk}\Lambda_{jk}\}, \qquad (1)$$

where n_j is the population density of state j (j runs over all levels including all ionisation stages), A is the spontaneous transition probability and Λ (depending on the photon effective path length L_{eff}) is the radiation transport term (currently approximated by means of an escape factor technique [7], including the spatial dependence $[n_j = n_j(\vec{r})]$, via the first-order approximation to the Bibermann–Holstein solution). The elements of the collisional-radiative transition matrix W are given by

$$W_{ij} = C_{ij} + R_{ij} + I_{ij} + T_{ij} + \Gamma_{ij} + D_{ij}, \qquad (2)$$

where C denotes the collisional excitation/deexcitation rate, I is the collisional ionisation rate, T is the 3-body recombination rate, R is the (spontaneous) radiative recombination rate, Γ is the auto-ionisation rate, and D is the radiationless electron capture rate. The matrix elements (rate coefficients or cross-sections) for the inverse processes are obtained by the application of the principle of detailed balance (or micro-reversibility). If a particular transition cannot occur, because of energy or symmetry considerations, the corresponding rate is set equal to zero.

The SOPHIA-code has several important properties. First, the energy level structure separates the relevant metastable levels as well as the singlet and triplet levels

for neutral helium up to arbitrary high n-quantum numbers while maintaining the full collisional-radiative processes between them. Therefore, any effects of incomplete thermalization caused by insufficient density and/or diffusion processes can be studied. The following levels are included: bare ion, H-like $1s^2S_{1/2}$, $2s^2S_{1/2}$, $2p^2P$, nl for $n = 3$–20, He-like levels $1s^2\,^1S_0$, $1s2s\,^1S_0$, $1s2s\,^3S_1$, $1s2p\,^1P_1$, $1s2p\,^3P$, $1snl\,^1L$ and $1snl\,^3L$ for $n = 3$–20.

The second important feature of SOPHIA is connected with the atomic data which are used in the simulations. Quantum mechanical calculations of cross-sections and rate coefficients have been performed up to high quantum numbers and scaling laws are derived for atomic structure and cross-sections for any arbitrary high n. Unlike the usual procedure in collisional-radiative modelings, we have taken into account also the intercombination transitions $1snl\,^1L$–$1sn'l'\,^3L$ and $1snl\,^3L$–$1sn'l'\,^1L$ by using a modified Multi-Configuration-Dirac–Fock method [8,9]. From these calculations, appropriate scaling rules were derived and the data for all transitions up to n, $n' = 1$–20 were implemented into the kinetic calculations.

Third, radiation transport effects are included self-consistently (causing Eq. (1) to be non-linear) for all levels and ionisation stages. Diffusion processes are calculated in τ-approximation, i.e., the flux divergence term $\nabla(n_j V)$ is replaced by $\frac{n_j}{\tau}$, i.e., loss terms for the ground states $1s^2$, 1s and nucleus are included in Eq. (1). At present, $\partial/\partial t = 0$ is assumed and the system Eq. (1) is closed by normalization conditions (for more details see [10,11]):

$$\sum_{i,k} n_{i,k} = 1. \tag{3}$$

The indices run over all ionisation stages k (He^{2+}, He^{+}, He^{0+}) and all levels i present in the kinetic Eq. (1). One dimensional numerical calculations for a large set of diffusion coefficients and convective velocities indicate, that the τ-approximation is able to keep track even of the details of the emission spectrum from metastable levels [10,11].

The spectral distribution $I(\omega)$ of the line emission is calculated from the full set of level-population densities, the Voigt-profile escape factors, and the normalized, optically-thick line-profile functions Φ_{ij}:

$$I(\omega) = \sum_{i,j} I_{ij}(\omega) = \sum_{i,j} \hbar\omega_{ij} A_{ij} \Lambda_{ij} \Phi_{ij}(\omega). \tag{4}$$

In order to compare the experimental data with the simulation $I(\omega)$ and derive suitable diagnostics for real experimental conditions, we also have included the continuum emission, namely the free–free and free–bound transitions.

4. Intercombination transitions and diffusion

Fig. 2(a) shows the line intensity ratio $I(1s2s\,^1S_0$–$1s5p\,^1P_1)/I(1s2p\,^3P$–$1s8d\,^3D)$ as a function of the electron density n_e for an electron temperature of $kT_e = 5$ eV, $\tau = \infty$ (no diffusion), $L_{eff} = 0$ (no radiation transport). A strong dependence of the ratio for electron densities between 10^{11} cm^{-3} and 10^{13} cm^{-3} is seen. The dependence is connected with the fact that levels with different n-quantum numbers equilibrate at different densities. The equilibration itself is essentially driven by ionisation (from the $1snl\,^1L$ and $1snl\,^3L$ levels) and 3-body recombination processes (from the 1s-level). The dashed curve is calculated by switching off all the intercombination transitions between the excited states n, $n' > 2$, while the solid curve shows the full calculations. The decrease of the dashed curve arises from the inclusion of the radiative intercombination transitions of the high n-states which results in a lower radiative branching ratio of

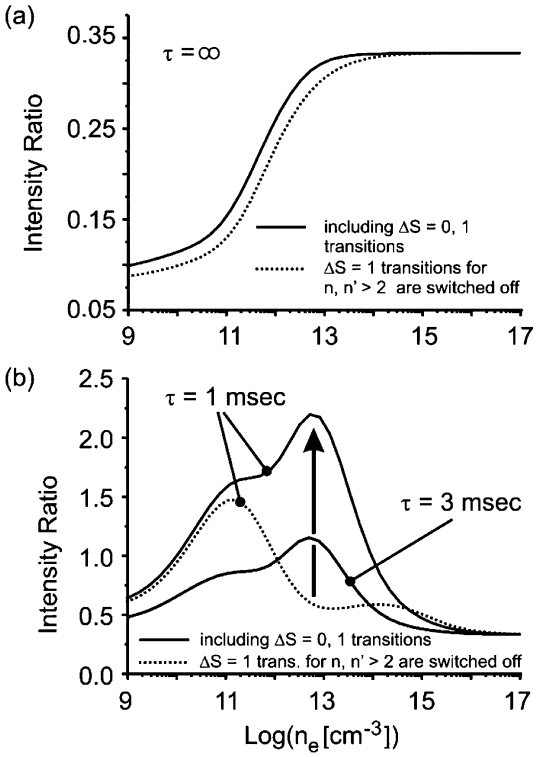

Fig. 2. SOPHIA simulation of the line intensity ratio $I(1s2s\,^1S_0$–$1s5p\,^1P_1)/I(1s2p\,^3P$–$1s8d\,^3D)$ in dependence of the electron density n_e. Solid lines include intercombination transitions between all combinations of states, dashed lines exclude $\Delta S = 1$ transitions for n, $n' > 2$ (see text), $kT_e = 5$ eV, (a) no diffusion, (b) diffusion time of $\tau = 1$ ms and 3 ms. The arrow indicates the great influence of intercombination transitions in the case of diffusion ($\tau = 1$ ms) and the variation of the intensity ratio for different diffusion times.

the triplet levels (about 10%). With increasing density, intercombination collisional processes provide a faster equilibration between the singlet and the triplet levels.

Fig. 2(b) shows calculations for the line ratio of Fig. 2(a) for the diffusive case $\tau = 1$ ms. It can be seen, that (unlike Fig. 2(a)) there is a large difference (indicated by arrow) between the solid and the dashed curves for $\tau = 1$ ms. The rise in the ratio is essentially connected with an effective collisional transfer from the triplet to the singlet levels. In the diffusive case, this process is much more important, because the diffusion reduces the thermalization processes (perturbation of the equilibrium relations which are established due to ionisation and 3-body recombination processes). Therefore, the difference of the populations between, e.g., the $1s51\,^1L$ and $1s51\,^3L$ levels is larger in the diffusive than in the non-diffusive case and collisions between these levels are much more important than for the case discussed in Fig. 2(a).

The sensitivity of the line ratio versus diffusion processes can be seen from Fig. 2(b), solid lines indicate the full calculations (including intercombination transitions) for $\tau = 1$ ms and $\tau = 3$ ms. Comparing with Fig. 2(a) we find, that the sensitivity to diffusion on the proposed ratio is very large for $\tau < 10$ ms.

Fig. 3 shows simulations for different electron temperatures in the case of diffusion, $\tau = 1$ ms. It can be seen, that the principle behaviour of the ratio (an increase near an electron density of 10^{13} cm^{-3}) is maintained for all electron temperatures. For higher electron temperatures the curves are broader due to ionisation balance effects which are more pronounced in the case of diffusion for high temperatures.

Comparison of the simulation results of Fig. 2(a) and (b) with the data of Fig. 1(a) and (b) shows, that the strong relative emission of the singlet $1s2s\,^1S–1s5p\,^1P$ line is obviously connected with non-equilibrium effects.

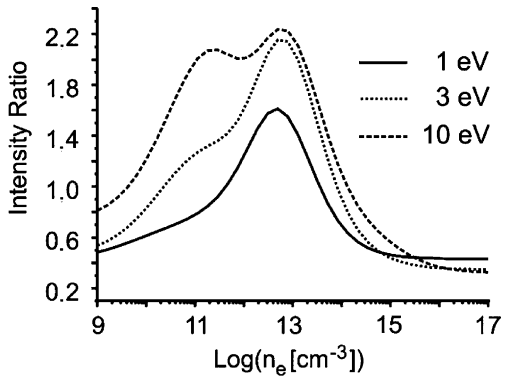

Fig. 3. SOPHIA simulation of the line intensity ratio $I(1s2s\,^1S_0–1s5p\,^1P_1)/I(1s2p\,^3P–1s8d\,^3D)$ for a diffusive plasma, $\tau = 1$ ms, in dependence of the electron density n_e for different electron temperatures, $kT_e = 1$, 3, 10 eV.

Ratios in the range of about 2 can be caused by diffusion effects. For the data presented in Fig. 1, the additional gas-puff leads to a relative overpopulation of the He-like ground state $1s^2$ (compared to the 1s-state) resulting in a relative decrease of the 3-body contribution for the population of the triplet-levels relative to the collisional excitation channel from the ground state (channels $1s^2–1snl\,^1L$ and $1s^2–1snl\,^3L$). Therefore the relative intensity of the triplet-series ($1s2p\,^3P–1snd\,^3D$) decreases, or in other words, the singlet line increases relatively to the triplet lines. In the simulation, this effect is taken into account by means of the diffusion time τ in Eq. (1) and the normalisation condition (Eq. (3)). The simulation is therefore able, to quantify the non-equilibrium situation of detached plasmas.

Employing spectral simulations in the wavelengths interval of 340–380 nm rather than only the single line ratios will finally constitute the diagnostic method to determine edge plasma conditions: from the Rydberg series, the electron density can be obtained via a Stark broadening analysis and from the continuum emission and recombination steps the electron temperature can be obtained. These parameters will be then used as input parameters to determine the diffusion coefficient from the proposed line ratios.

5. Conclusion

Line emission from neutral helium has been investigated experimentally and theoretically for diffusion effects for edge plasma conditions. We have shown that the intensity of transitions originating from the singlet and triplet system strongly depends on diffusion. The simulations indicate, that collisional and radiative intercombination transitions are very important for the description of the line emission in diffusive plasmas whereas in equilibrium plasmas the effects are much smaller.

References

[1] N. Ohno, D. Nishijima, S. Takamura, et al., Nucl. Fus. 41 (2001) 1055.
[2] A. Escarguel, B. Pegourié, J. Hogan, et al., Plasma Phys. Control. Fus. 43 (2001) 1743.
[3] R. Guirlet, M. Koubiti, A. Escarguel, et al., Plasma Phys. Control. Fus. 43 (2001) 177.
[4] F.B. Rosmej, SOPHIA-code, in press.
[5] F.B. Rosmej, M. Koubiti, H. Capes, et al., Proc. of the 30th EPS Conf. on Plasma Physics, St. Petersburg 2003, ECA, vol. 27A, 2003, p. 1.176.
[6] S. Narita et al., in: Plasma Physics, vol. 2, The Japan Society of Plasma Science and Nuclear Fusion Research, Nagoya, p. 1362, Proc. Int. Conf. Nagoya, 1996.
[7] F.E. Irons, JQSRT 22 (1979) 1.

[8] S. Fritzsche, J. Electron Spectrosc. Relat. Phenom. 114–116 (2001) 1155.
[9] S. Fritzsche, C. Froese-Fischer, C.Z. Dong, Comput. Phys. Commun. 124 (2000) 340.
[10] F.B. Rosmej, D. Reiter, V.S. Lisitsa, et al., Plasma Phys. Control. Fus. 41 (1999) 191.
[11] F.B. Rosmej, V.S. Lisitsa, Phys. Lett. A 244 (1998) 401.